Hindawi
Complexity
Volume 2018, Article ID 4154673, 13 pages
https://doi.org/10.1155/2018/4154673

Research Article

The Performance Study on the Long-Span Bridge Involving the Wireless Sensor Network Technology in a Big Data Environment

Liwen Zhang[1], **Chao Zhang**[1], **Zhuo Sun**[1], **You Dong**[2] and **Pu Wei**[3]

[1]*Department of Civil Engineering, Guangzhou University, Guangzhou, China*
[2]*Department of Civil and Environmental Engineering, Hong Kong Polytechnic University, Hong Kong*
[3]*Shanghai Municipal Engineering Design Institute, Shanghai, China*

Correspondence should be addressed to Chao Zhang; zhch2013@gzhu.edu.cn

Received 13 April 2018; Revised 22 May 2018; Accepted 29 May 2018; Published 26 June 2018

Academic Editor: Zhihan Lv

The random traffic flow model which considers parameters of all the vehicles passing through the bridge, including arrival time, vehicle speed, vehicle type, vehicle weight, and horizontal position as well as the bridge deck roughness, is input into the vehicle-bridge coupling vibration program. In this way, vehicle-bridge coupling vibration responses with considering the random traffic flow can be numerically simulated. Experimental test is used to validate the numerical simulation, and they had the consistent changing trends. This result proves the reliability of the vehicle-bridge coupling model in this paper. However, the computational process of this method is complicated and proposes high requirements for computer performance and resources. Therefore, this paper considers using a more advanced intelligent method to predict vibration responses of the long-span bridge. The PSO-BP (particle swarm optimization-back propagation) neural network model is proposed to predict vibration responses of the long-span bridge. Predicted values and real values at each point basically have the consistent changing trends, and the maximum error is less than 10%. Hence, it is feasible to predict vibration responses of the long-span bridge using the PSO-BP neural network model. In order to verify advantages of the predicting model, it is compared with the BP neural network model and GA-BP neural network model. The PSO-BP neural network model converges to the set critical error after it is iterated to the 226th generation, while the other two neural network models are not converged. In addition, the relative error of predicted values using PSO-BP neural network is only 2.71%, which is obviously less than the predicted results of other two neural network models. We can find that the PSO-BP neural network model proposed by the paper in predicting vibration responses is highly efficient and accurate.

1. Introduction

With the progress of the era, transportation and automobile industries have achieved rapid development, while vehicle loads acting on bridge structures also are increased continuously. As a result, the traffic flow will be increased continuously, driving speeds of vehicles will be increased obviously, and a lot of heavy-load vehicles travel on highway. In some regions, the overload phenomena are serious, and vehicle dynamic loads become one of the main reasons for bridge deck damage, threatening the safe of long-span bridges [1–5]. Vehicle loads of long-span bridges are significantly different from those of middle-span and small-span bridges, which are mainly reflected in the following aspects: main beams of long-span bridges have low rigidity, and the main beam deformation is obvious under vehicle loads; long-span bridges are mainly located at traffic throat positions with large traffic flow; long-span bridges are obviously affected by intensive vehicles. Strong traffic flow will lead to violent vibrations of bridges. Therefore, simulation research on loads acting on long-span bridge decks during traffic flow driving becomes one important issue in studying vehicle-bridge dynamic systems [6–8]. More and more obvious vehicle-bridge coupling vibration issues gradually cause attention of scholars. Aiming at numerical analysis on vehicle-bridge coupling vibrations of complicated bridges, Shi et al. [9] proposed a computational method for achieving vehicle-bridge coupling vibrations of complicated bridges on

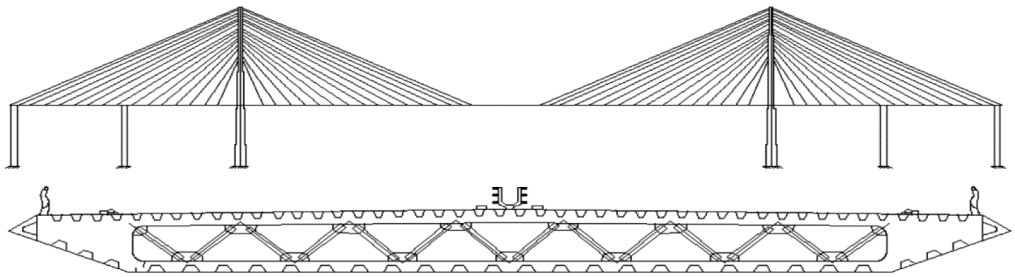

Figure 1: Schematic diagram of long-span bridges.

highways with finite element software, deeming vehicle and complicated bridge as two separate subsystems. Based on contact relations between wheels and bridge deck, Ji et al. [10] established a dynamic equation of vehicle-bridge coupling vibrations. With considering random excitation from road surface roughness, vehicles were deemed as certain loads, and responses of bridge node displacement were solved. Zhang et al. [11] solved random excitation caused by bridge deck roughness and certain excitation caused by gravity using a virtual excitation method; mean values and standard deviations of bridge midspan deflection and stress responses were finally obtained.

However, when vehicle loads are considered, they compute vehicle loads according to bridge design specifications and neglected randomness of traffic flows. Therefore, the obtained conclusions had a great deviation from results of the experimental test. Computational results will further approach actual engineering situations, and engineering practice can be guided better by studied conclusions if random traffic flow conditions can be investigated fully; comprehensive statistical analysis can be conducted to parameters; and a random traffic flow simulation program based on tested data can be compiled on this basis and used for studying bridge structures. Yin and Deng [12] fitted a function expression of influential faces according to a method of response face analysis and solved the maximum deflection of bridge structures under random traffic flow. Yin et al. [13] introduced a method of cellular automation for random traffic flow simulation, used an established whole-vehicle model which could consider spatial vehicle vibration to simulate heavy-type vehicles in traffic flows, used a single-freedom degree vehicle model to simulate other vehicle types in the traffic flow, and established a motion equation under coupling effects between bridges and traffic flows. Chen and Wu [14] have adopted the cellular automaton (CA) traffic flow simulation technique to simulate the actual traffic flow. Based on the traffic flow simulation results, the live load on a long-span bridge from the stochastic traffic is studied with a focus on the static component. Enright and O'Brien [15] have presented a comprehensive model for Monte Carlo simulation of bridge loading for free-flowing traffic and show how the model matches results from measurements on five European highways.

At present, researches on random traffic flow loads acting on bridges are mainly focused on statistical analysis theories, depend too much on basic assumption about unchanging of vehicle type, vehicle weight, vehicle distance, and vehicle speed, and fail to fully study and consider random characteristics of each traffic flow parameters. Aiming at such situation, this paper tests bridge health and monitors traffic flow parameters including vehicle type, vehicle weight, and vehicle speed. Then, through mathematic statistical analysis, representative data of traffic situations is obtained. Simulation on random traffic flow is conducted, and a random vehicle flow program is compiled on this basis. A vehicle-bridge coupling model including random traffic flows is established, which can consider vehicle type, vehicle weight, vehicle lane, vehicle speed, and opposite driving functions. After that, response values of the bridge structure are extracted to be compared with tested values. In the testing, tested time is long, so there are many data parameters to be monitored. Size of data to be uploaded to the data center will be very huge. In view of the large bridge spans, monitoring with traditional wired sensor networks must be confronted with long wiring and high monitoring difficulty. Thanks to rapid development of big data analysis technology, microcomputer system, sensor technology, wireless communication technology, and low-power consumption embedding technology, it is possible to acquire and process data with a wireless sensor network. With increase of monitoring scope and monitoring points, the data throughout to be realized by the network shall be increasingly higher. Finally, massive data will be uploaded to the data center, belonging to the category of big data. The computational results are practical and reliable. The vehicle-bridge coupling vibration model with considering random traffic flows established in the paper is feasible.

2. Computational Model of Long-Span Bridges

This paper selected a long-span bridge with two towers as the studied object, as shown in Figure 1. Span is as follows: 160 m + 160 m + 426 m + 160 m + 160 m = 1066 m. Upper and lower inclined webs are set on the fracture section to form a wind guide nozzle. The total height of cable tower is 170.3 m, and the horizontal distance between two cable towers is 426 m. The cable tower main body is made of concrete and forms an H-shaped tower. Compared with common steel bridge structures, long-span bridges are more complicated. Consolidation is the form of tower bridge integration.

According to size parameters in Figure 1, a finite element model of the long-span bridge was established by ANSYS. Basically, the cross section of main beams can be deemed to be longitudinally unchanged [16]. Beam4 elements were used

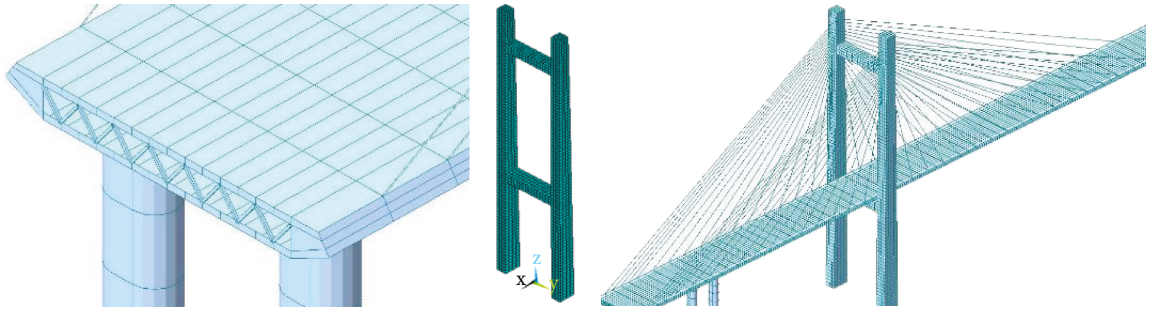

(a) Cross section (b) Cable tower (c) Stay cable

Figure 2: Local mesh model of long-span bridges.

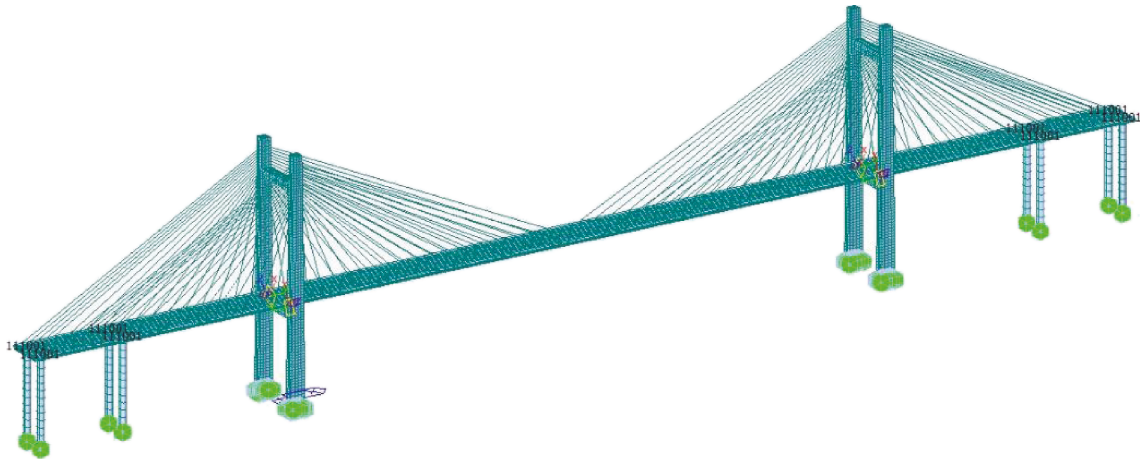

Figure 3: Boundary constraints of long-span bridges.

to simulate stiffening beams and cable towers. Mass21 elements were used to simulate torsion inertia moment and additional bridge deck mass. Cable towers, piers, and beams are connected by a coupled node method. Gravity rigidity of the long-span bridge has a significant impact on structural rigidity. In order to ensure the reliability of computational results, accurate structure materials should be set. Finally, 4639 nodes and 8741 elements were divided for the complete bridge. Local model of the long-span bridge was extracted, as shown in Figure 2. It is shown in this figure that meshes of the finite element model were relatively regular.

Connections between cable tower, pier, and girder are as follows: CP command of nodes in ANSYS was used to couple three translational freedom degrees and three rotational freedom degrees between two nodes. The cable towers and piers were processed by the complete consolidation, so freedom degrees in 6 directions were restrained, as shown in Figure 3. Finally, vibration shapes of top 7 orders of the bridge can be extracted, as shown in Figure 4. Modal frequencies are 0.32 Hz, 0.39 Hz, 0.45 Hz, 0.72 Hz, 0.82 Hz, 0.91 Hz, and 1.07 Hz, respectively. Obviously, the frequencies are distributed densely, satisfying the feature of dense distribution of natural frequencies of large infrastructures. In addition, it is shown in this figure that the first-order vibration shape is mainly reflected by bending vibration of cable towers and bridge deck; the second-order vibration shape is mainly reflected by bending vibration of cable towers; the third-order vibration shape is mainly reflected by second-order bending vibration of the beam; the fourth-order vibration shape is mainly reflected by bending vibration of beams and piers; the fifth-order vibration shape is reflected by bending and torsion coupling vibration of the beam; and vibration shapes of other orders are mainly reflected by bending and torsion vibration of beams and cable towers as well. Therefore, vibration shapes of the long-span bridge are not completely the simple torsion or bending vibration. Sometimes, the vibration shapes are overlaid results of these two vibration shapes.

3. Vibration Responses of Long-Span Bridges

3.1. Road Surface Roughness. The paper will study vehicle-bridge coupling vibration responses. Therefore, bridge deck roughness should be input into the computational model. Bridge deck roughness refers to deviation levels of the bridge surface relative to a standard plane. According to a lot of experimental results, bridge deck roughness is an argotic and steady Gauss random process with a mean value of zero. Therefore, it could be simulated by different forms of trigonometric series. Within the spatial frequency scope of $n_1 < n < n_2$, the power spectrum density of bridge deck roughness is $G_q(n)$. Based on a frequency spectrum

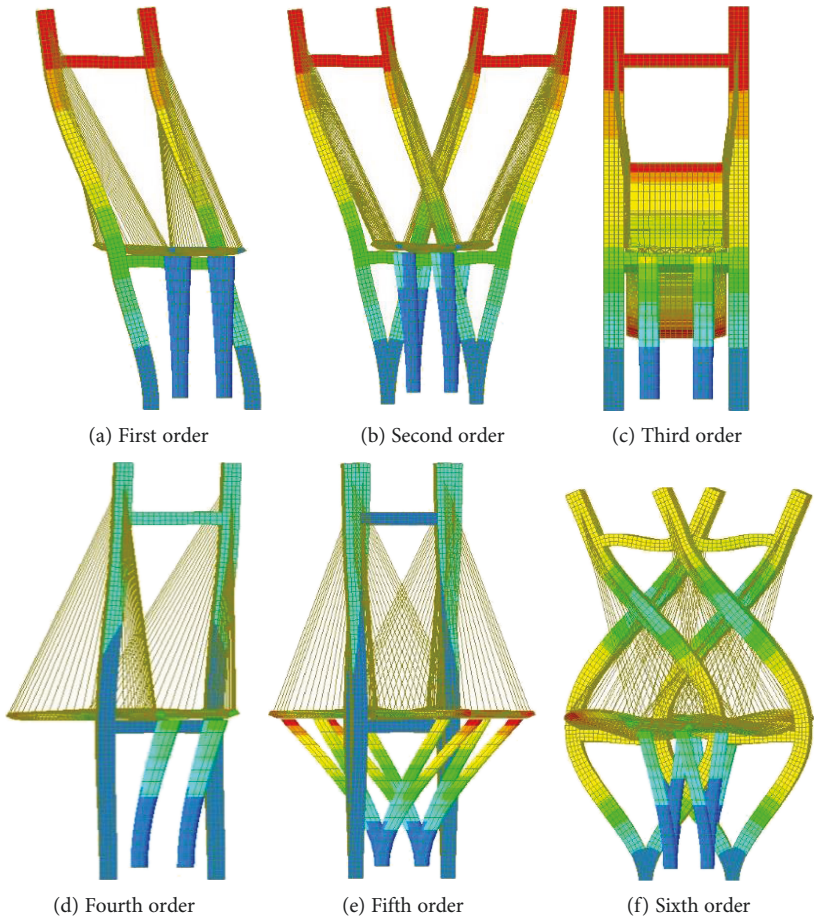

Figure 4: Modal vibration shapes of top 7 orders for long-span bridges.

spreading form of the steady random process, the variance σ_q^2 of the bridge deck roughness could be expressed by [17–21]

$$\sigma_q^2 = \int_{n_1}^{n_2} G_q(n)dn. \tag{1}$$

Fitting expression of power spectrum density $G_q(n)$ of the bridge deck roughness is as follows:

$$G_q(n) = G_q(n_0)\left[\frac{n}{n_0}\right]^{-w}, \tag{2}$$

where n is spatial frequency; n_0 is referential space frequency; $G_q(n_0)$ is a bridge deck roughness coefficient; $G_q(n)$ is displacement power spectrum density; and w is a frequency index and $w = 2$. As for integral operation in (1), the scope $n_1 < n < n_2$ of spatial frequency can be divided into m small intervals. Width of each small interval is Δn_i. The roughness power spectrum density value $G_q(n_{\mathrm{mid},i})$ at the center frequency $n_{\mathrm{mid},i}$ $(i = 1, 2, \ldots, m)$ of each small interval is used to replace the $G_q(n)$ value in the complete spatial frequency scope $n_1 < n < n_2$. Therefore, (1) can be rewritten into

$$\sigma_q^2 = \sum_{i=1}^{m} G_q(n_{\mathrm{mid},i})\Delta n_i. \tag{3}$$

Through comparing (1) and (3), we can find that (3) is integral in (1) using a discrete form. Hence, the computational accuracy is affected to a certain extent. However, through rational value option of the discrete interval, the computational error can be controlled within an allowable scope. In order to obtain the random bridge deck roughness, a sine wave function with spatial frequency of $n_{\mathrm{mid},i}$ $(i = 1, 2, \ldots, m)$ and standard deviation of $(G_q(n_{\mathrm{mid},i})\Delta n_i)^{1/2}$ is used to denote the bridge deck model. The sine wave function can be denoted as follows:

$$q_i(x) = \sqrt{2G_q(n_{\mathrm{mid},i})\Delta n_i}\,\sin\,(2\pi n_{\mathrm{mid},i}x + \theta_i). \tag{4}$$

Sine wave functions corresponding to different intervals are overlaid, so a random bridge deck roughness model can be obtained.

$$q(x) = \sum_{i=1}^{m} \sqrt{2G_q(n_{\mathrm{mid},i})\Delta n_i}\,\sin\,(2\pi n_{\mathrm{mid},i}x + \theta_i). \tag{5}$$

Formula (5) gives an expression of random bridge deck roughness obtained by sine wave overlaying, where θ_i is a random number; x is determined according to the longitudinal position; the discrete interval size Δn_i can be set according to the experience; each interval can be assumed to have

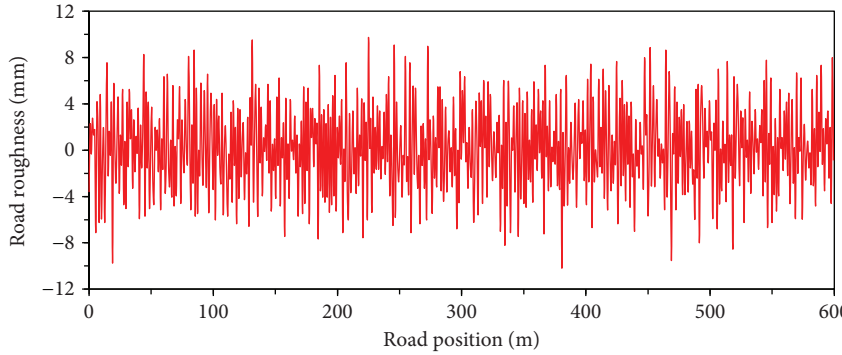

Figure 5: Bridge deck roughness of long-span bridges.

the equal size. $n_{\text{mid},i}$ is the center frequency of each interval, which can be obtained according to the interval size Δn_i and the initial spatial frequency scope $n_1 < n < n_2$. $G_q(n_{\text{mid},i})$ can be computed by (2). According to above computation requirements, the MATLAB software was used to compile the bridge deck roughness under given conditions, as shown in Figure 5. It is shown in this figure that the bridge deck is not completely smooth, and the maximum roughness approaches 10 mm. In this paper, we only studied the dynamic response of towers and piers at the left side of the long-span bridge. These two positions of the long-span bridge are less than 600 m. Therefore, the length of the road roughness is reasonable.

3.2. Random Traffic Flow in a Big Data Environment Using the Wireless Sensor Networks. The paper researches vibration responses of bridges under random traffic flow, so random traffic flows need to be monitored. When vehicles run on a bridge, the vehicle speeds, vehicle types, vehicle distances, vehicle weights, and lanes would change randomly. All these parameters shall be taken into account. Monitoring time is long, so there are many data parameters to be monitored. Size of data to be uploaded to the data center will be very huge. In view of the large bridge spans, monitoring with traditionally wired sensor networks must be confronted with long wiring and high monitoring difficulty. Thanks to the rapid development of big data technology [22, 23], microcomputer system, sensor technology, wireless communication technology [24, 25], and low-power consumption embedding technology, it is possible to acquire and process data with a wireless sensor network [26, 27]. A wireless sensor network is composed of micro and flexible sensor nodes distributed in a monitoring area and transmits information of collecting objects to a processing system through wireless communication, so the collector can analyze and use the information. Advantageous in micro size, low cost, high flexibility, and so forth, wireless sensor networks have been applied to many fields such as military reconnaissance, environmental monitoring, medical health, intelligent transportation, smart grid, and building monitoring, as shown in Figure 6. Random traffic flow parameters on a long-span bridge are monitored in the paper, wherein they are featured by large covering scope and a lot of data collection points, as shown in Figure 7. According to the length of the long-span bridge and the characteristics of these sensors, we have arranged 24 sensors in the experimental test. Four sensors are connected to one sink node, and 3 sink nodes are connected to one base station. According to different monitoring objects and purposes, there are many types of monitored data. Hence, the monitored data shall be uploaded to the monitoring center in time and shall be summarized and analyzed by the monitoring center in real time. Because of these characteristics, the wireless sensor network shall guarantee high efficiency of data transmission. With increase of monitoring scope and monitoring points, the data throughout to be realized by the network shall be increasingly higher. Finally, massive data will be uploaded to the data center, belonging to the category of big data. Further, analysis and statistics are conducted to the mass data. On this basis, random traffic flows can be generated for bridge analysis. In order to validate the subsequent simulation, the dynamic response of the long-span bridge should be tested, so that we have also placed some tested points on the cable tower and pier.

When the random traffic flow was obtained, we have prepared a program to use the random traffic flow. In the program, the vehicle lane, vehicle type, vehicle weight, vehicle speed, and roughness spectrum were considered. Finally, the prepared program was combined with the ANSYS software because ANSYS can output the command script file. Detailed methods, steps, and processes of numerical analysis on vehicle-bridge coupling vibration based on ANSYS are shown in Figure 8. At first, a structural finite element model of long-span bridges is established; structural information of the bridge is input; corresponding mass and rigidity matrixes are obtained. The above random traffic flow model which considers parameters of all the vehicles passing through the bridge, including arrival time, vehicle speed, vehicle type, vehicle weight, and horizontal position as well as the bridge deck roughness, is input into the vehicle-bridge coupling vibration program. In this way, vehicle-bridge coupling vibration responses with consideration of the random traffic flow can be obtained in the ANSYS software.

3.3. Analysis and Discussion on Vibration Responses. Vibration displacements and accelerations at cable towers and piers of the long-span bridge are computed, as shown in Figure 9. In this paper, we have only concerned the dynamic

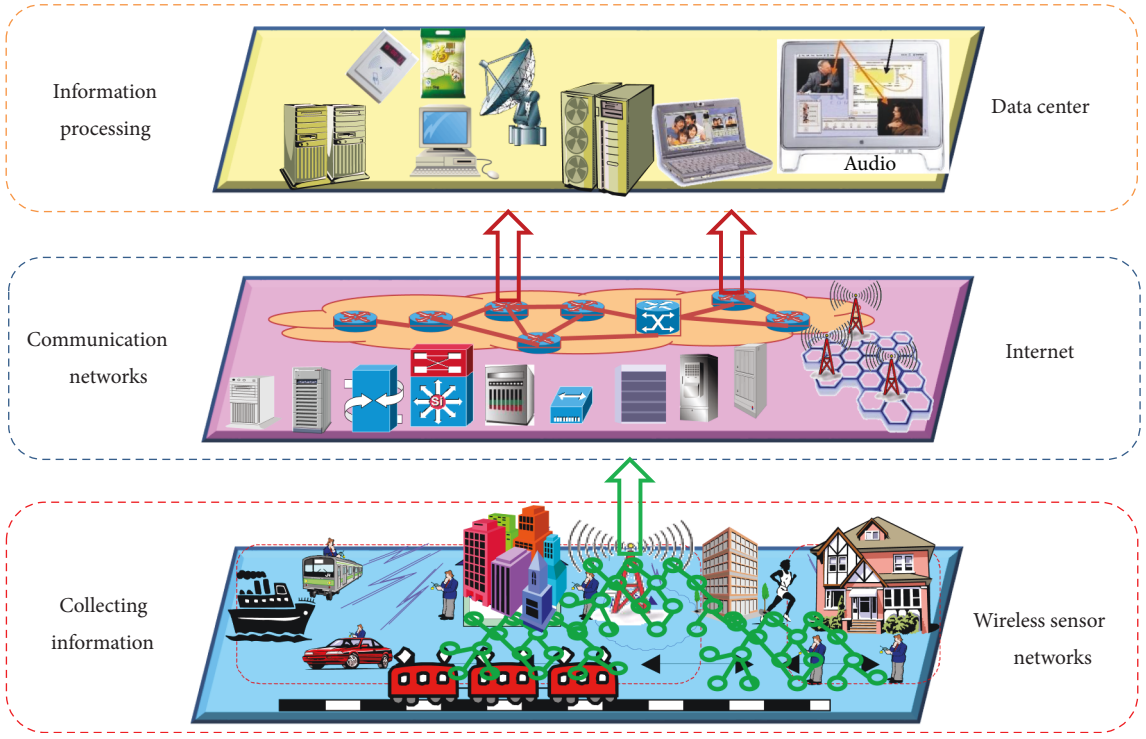

Figure 6: Application of the wireless sensor network.

response at the cable tower and pier because there are a lot of reported papers which have studied the dynamic response at the bridge surface, and dynamic responses at the cable tower and pier were rarely reported. It is shown in this figure that vibration displacements and accelerations at the cable tower are obviously more than those at piers. The pier is a round structure made of reinforced concrete. It has the biggest rigidity among all the structures and will generate the minimum responses to vehicle loads.

4. Experimental Verification of the Computational Model of Long-Span Bridges

Such complicated model of the long-span bridge is affected by many parameters, so its correctness should be verified by experimental test. As shown in Figure 7, the wireless sensor network technology is used to test the dynamic response of the long-span bridge under random traffic flow. In the testing process, the wind speed is very small, so its impact can be neglected. Time domain vibration displacements of experimental test are compared with numerical simulation results, as shown in Figure 10. It is shown in this figure that experimental results and numerical simulation results basically had the consistent changing trends. At some peaks, experimental values are slightly more than numerical simulation results. The reason is that boundary conditions of the numerical simulation are relatively ideal states and only consider effects of random traffic flow on the bridge, but they neglect actual wind excitation. In addition, material characteristics of the numerical simulation can hardly be kept consistent with actual values. Wind speeds in experimental test are low, and excitation borne by the bridge is mainly generated from vehicles, so results between numerical simulation and experimental test do not have big errors. This result proves the reliability of the vehicle-bridge coupling model in the paper.

5. Prediction of Vibration Responses for Long-Span Bridges Based on the PSO-BPNN Model

As mentioned, vibration responses of the long-span bridge are computed using finite element simulation. However, the computational process of this method is complicated and proposes high requirements for computer performance and resources. Therefore, the paper considers using a more advanced intelligent method to predict vibration responses of the long-span bridge. BP neural network model is a typical multilayer feed forward neural network. With a strong capacity of information classification and recognition, it can achieve approximation problem of any function [28–31]. It performs very well in self-learning, self-organization, fault tolerance, and nonlinear mapping, so it is widely applied in scientific and technological fields. A typical BP network is composed of three layers including input layer, hidden layer, and output layer. One or more than one hidden layer may be set. As for network structure, nerve cells between the upper layer and the lower layer are not connected. Each unit of the lower layer is completely connected to each unit of the upper layer. Nerve cells on each layer are not connected. Increase of the hidden layers can reduce errors and increase training accuracy. But as a result, the network will become complicated and the network operation time will be too long. When only one hidden layer is set, the accuracy will be

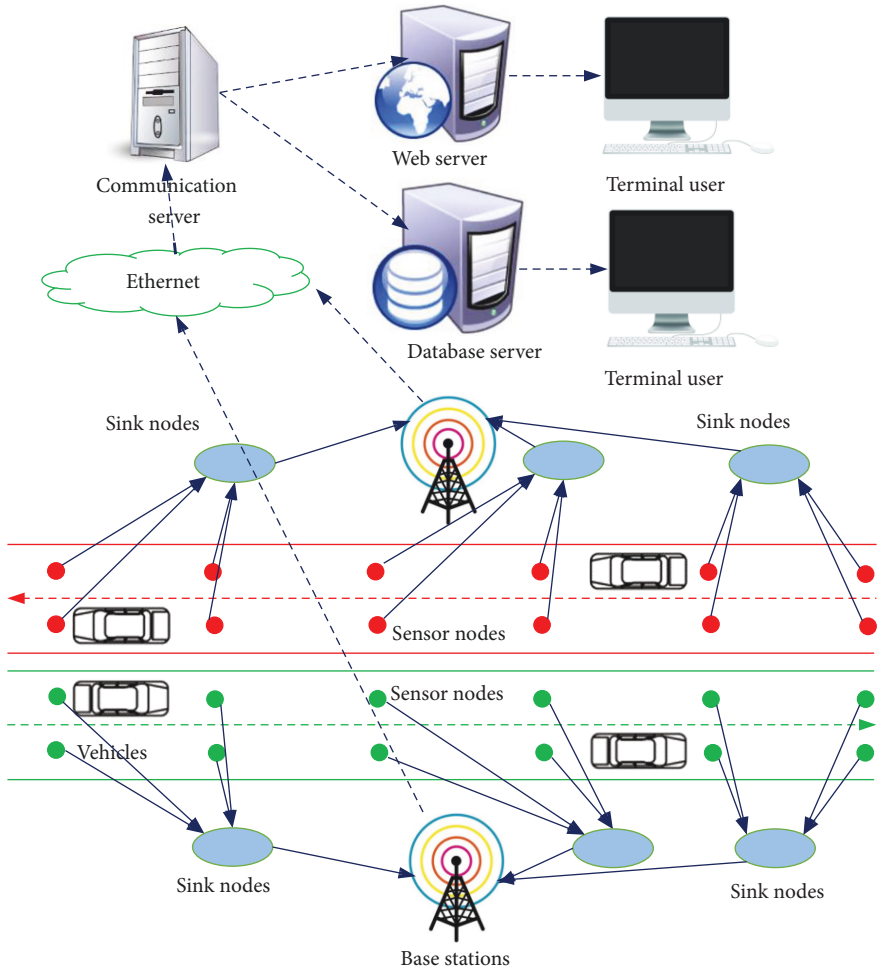

Figure 7: Collection of random traffic flow loads using the wireless sensor network.

low, and the network generalization ability will be weak. Therefore, the quantity of hidden layers in a network must be selected rationally according to complexity degree of mapping relations in actual issues, with network training accuracy and network operation speed as the selected standards.

BP neural work is widely applied in many fields and also achieves some effects [32–34]. However, results are not very ideal sometimes in practical application. There are still some problems as follows: (1) Training speed of the BP neural network is too slow. A relatively simple model may be converged to the set error accuracy through multiple times of training. (2) Convergence to the global minimum value cannot be ensured. (3) Selection of hidden layer and node quantity does not have a scientific basis. The quantities can only be determined according to an empirical formula. Hence, the structure is big and complicated with large redundancy. Convergence time of the algorithm will be longer. (4) Learning and memorization of networks are not stable. (5) Generalization problem of learned networks exists, namely, whether rules can be approximated and whether a lot of unlearned input vectors will be processed correctly. Aiming at mentioned defects of BP neural network, experts and scholars in the artificial intelligent field have made a lot of researches and proposed many improvement proposals to increase convergence speed of BP network and reduce the possibility of getting trapped in local minimum values. For example, a particle swarm optimization algorithm can be introduced to optimize the BP neural network or improve the BP neural network learning algorithm so as to achieve improvement or supplement.

Particle swarm optimization (PSO) algorithm is an optimization algorithm based on swarm intelligence theories and is also an effective global optimization algorithm [35–38]. PSO is featured by evolutionary techniques and group intelligence, where the optimum solution in complicated space is searched through cooperation and competition between particles in a group. Compared with a traditional evolutionary algorithm, PSO adopts a speed displacement model with simple operations and inherits the global search strategy based on groups. Because of the memorization function, each particle can store good search conditions, and optimization ability can be improved. PSO algorithm is a global optimization algorithm. It is featured by very simple concepts, fewer parameters, easy realization, high global search ability, high robustness, and so on Hence, PSO and BP neural networks have very high complementarily. At present,

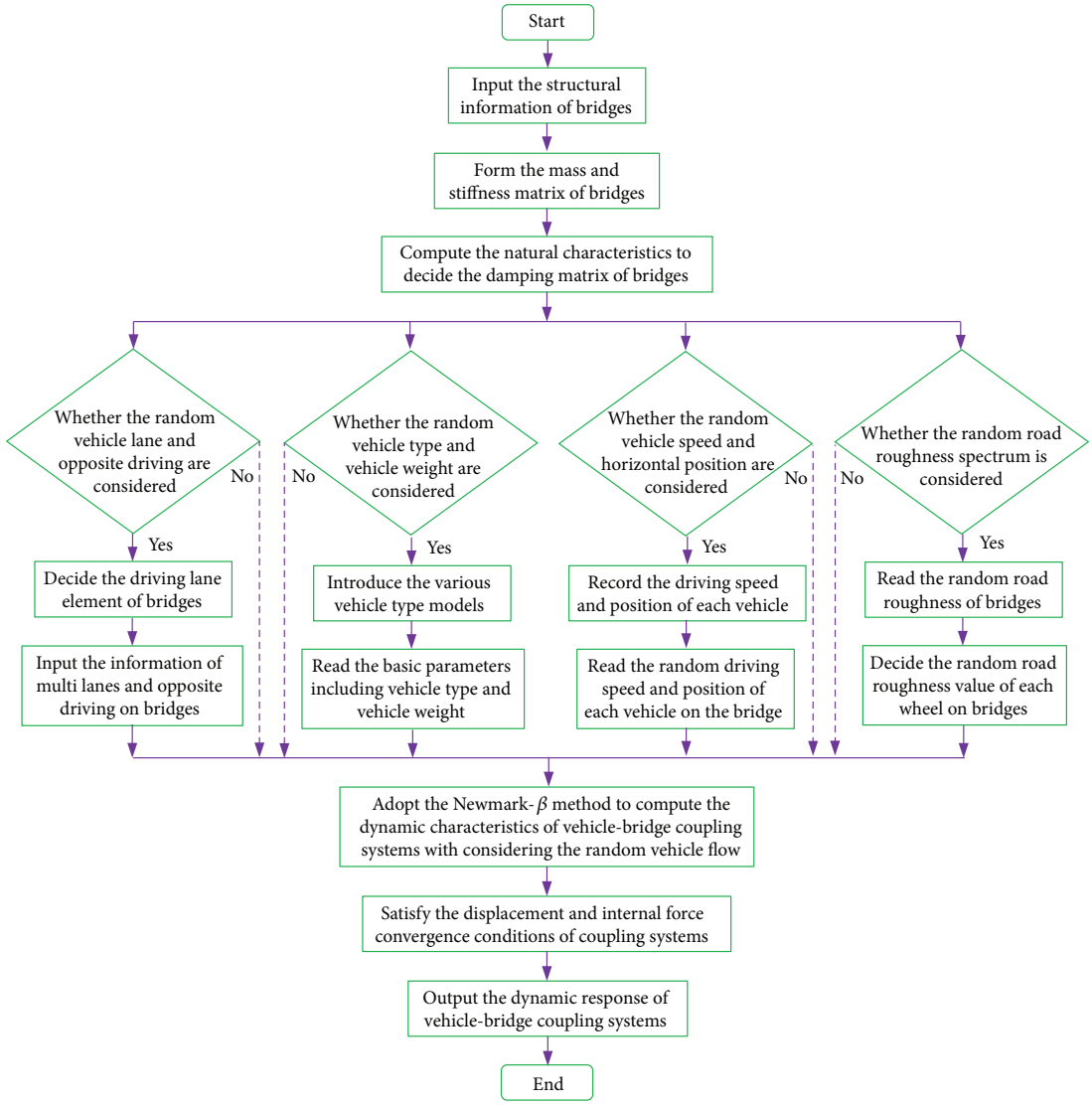

Figure 8: Solution processes of vehicle-bridge coupling vibrations.

optimization of BP neural network using the particle swarm algorithm mainly involves the following two aspects, namely, optimization of network connection weights and thresholds and optimization of a network topology structure. Compared with the optimization of network weights and thresholds, optimization of a network structure is complicated. Besides, changes of the network structure will affect dimensional changes of PSO solution space. Therefore, its realization is difficult, and convergence speed of the algorithm will be affected. For above reasons, the paper selects the first type to optimize BP neural network, as shown in Figure 11.

The PSO-BP neural network model is used to predict vibration responses of the long-span bridge. Vibration responses obtained by numerical computation in Section 4 are divided into two parts. The first part is vibration responses of the first 30 min, which is used to train the PSO-BP neural network model as training data, as shown in Figure 12. It is shown in Figure 12 that after 30 min of training, the performance of PSO-BP neural network model becomes stable. Therefore, the trained model can be used to predict vibration responses of the last 30 min. Predicted results are compared with real values, as shown in Figure 13. Figure 13 presents comparison between predicted values and real values of vibration responses at cable tower and pier of the long-span bridge. It is shown in Figure 13 that predicted values and real values of the neural network at each position point basically have the consistent changing trends; only some peak values are different; the maximum error of predicted values is less than 10%. Hence, it is feasible to predict vibration responses of the long-span bridge using the PSO-BP neural network model.

In order to verify advantages of the prediction model, we have extracted the predicting process of the vibration displacement at cable tower using the PSO-BP neural network model. Then, it is compared with the BP neural network model and GA-BP neural network model, as shown in Table 1. In fact, the compared algorithms BPNN and GA-

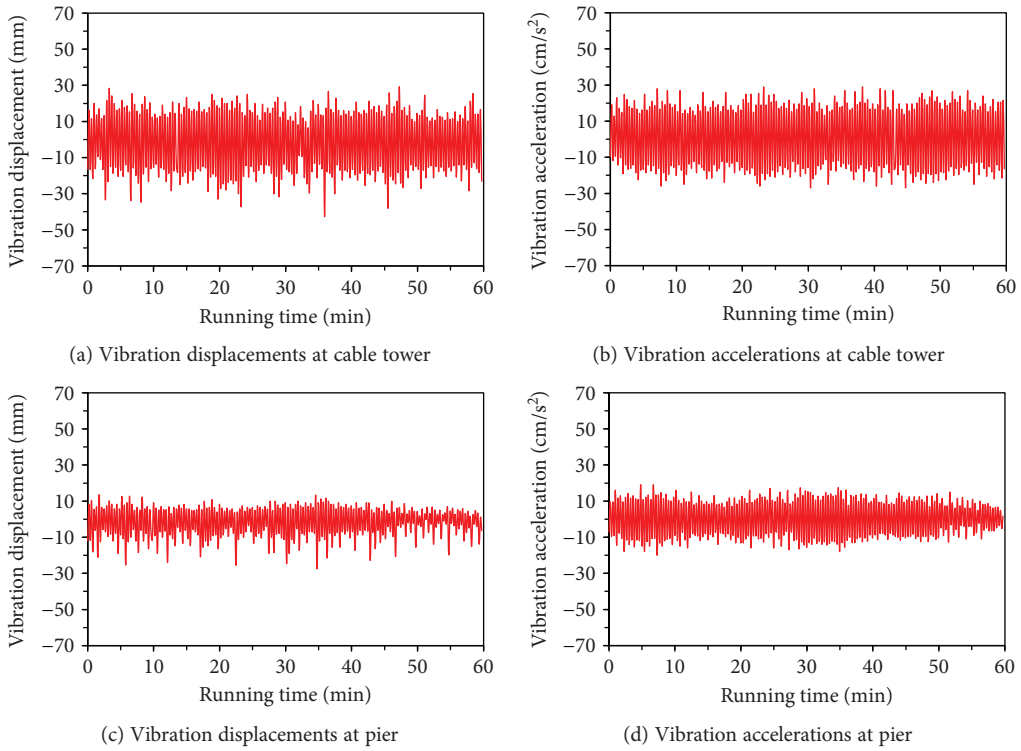

(a) Vibration displacements at cable tower

(b) Vibration accelerations at cable tower

(c) Vibration displacements at pier

(d) Vibration accelerations at pier

Figure 9: Vibration responses at different positions of long-span bridges.

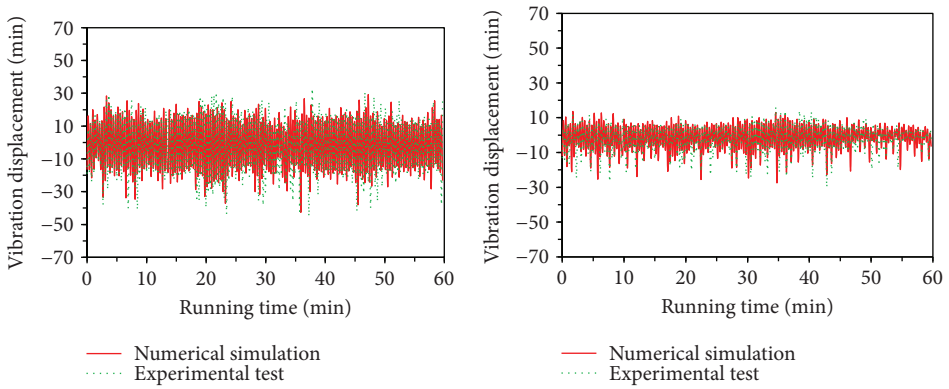

(a) Vibration displacements at cable tower

(b) Vibration displacements at pier

Figure 10: Comparison of bridge vibration responses between experiment and simulation.

BPNN models are not the most advanced, but they have been widely used in many engineering. Additionally, BPNN and GA-BPNN models have the same topology structure with the proposed PSO-BPNN model, so they can form a valid comparison with the proposed PSO-BPNN model. The termination condition for training iterations of three kinds of neural network models is to reach the set critical error 0.016 or the maximum iteration 500. It is shown in Table 1 that the PSO-BP neural network model converges to the set critical error after it is iterated to the 226th generation, whereas at this moment, the other two neural network models are not converged. The reason is that PSO can accelerate convergence of the neural network model. The training errors are 0.08 and 0.016, respectively, when the BP neural network reaches the maximum iteration 500, and GA-BP neural network reaches the 398th generation, but errors using the BP neural network are still more than the set critical error 0.016. During the complete iteration, both neural network models get trapped in local extremes and cannot jump out, so iterations are repeated. Therefore, the complete process of training and prediction is time-consuming. The PSO-BP neural network model can effectively avoid local extremes and search global optimal values, so that it is least time-consuming in the complete process. In addition, it is shown in Table 1 that the relative error of predicted values of PSO-BP neural

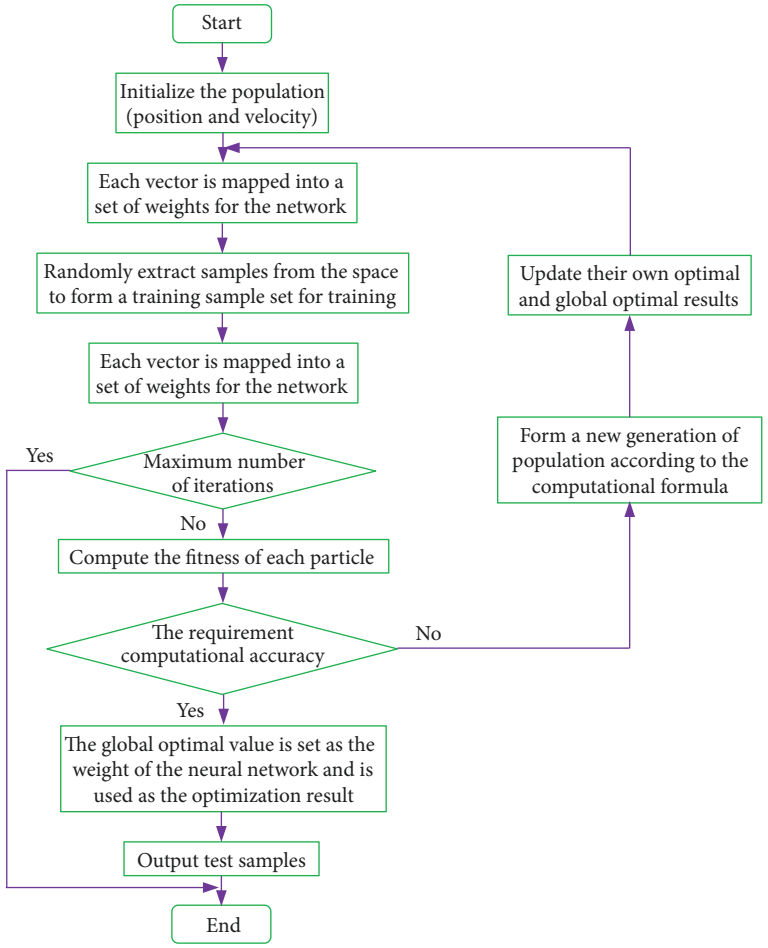

Figure 11: Flow chart of PSO-BP neural network model.

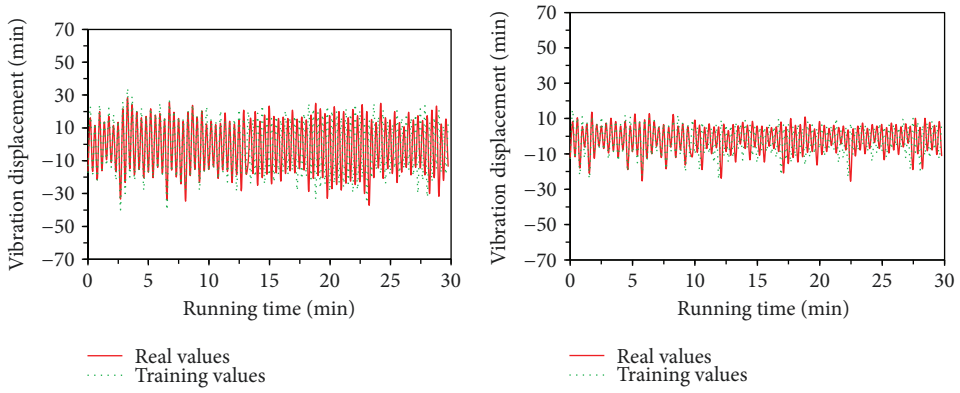

(a) Vibration displacements at cable tower

(b) Vibration displacements at pier

Figure 12: Training of PSO-BP neural network model.

network is only 2.71%, which is obviously less than the predicted results of other two neural network models. Also, the predicting time using PSO-BP neural network model is less than the other two kinds of algorithms, as shown in Table 1. According to above analysis, we can find that application of the PSO-BP neural network model proposed by the paper in predicting vibration responses is highly efficient and accurate.

6. Conclusions

(1) Modal frequencies of the long-span bridge are 0.32 Hz, 0.39 Hz, 0.45 Hz, 0.72 Hz, 0.82 Hz, 0.91 Hz, and 1.07 Hz, respectively. Obviously, the frequencies are distributed densely, satisfying the feature of dense distribution of natural frequencies of large infrastructures. In addition, vibration shapes of the long-span

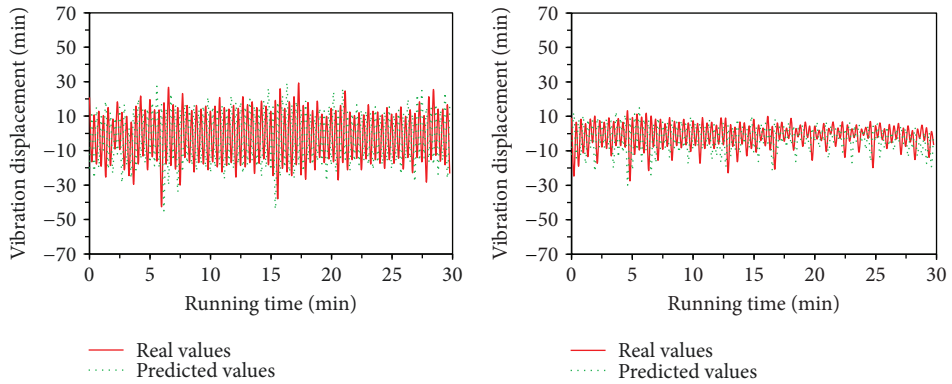

(a) Vibration displacements at cable tower

(b) Vibration displacements at pier

Figure 13: Prediction of PSO-BP neural network model.

Table 1: Comparison of predicted results for three kinds of neural network models.

Predicting algorithms	Training errors	Amount of iterations	RMS of predicted results (mm)	Real results (mm)	Relative errors (mm)	Predicting time
BPNN	0.08	500	20.1	18.4	9.23	1.05 hours
GA-BPNN	0.016	398	19.2	18.4	4.34	0.70 hours
PSO-BPNN	0.016	226	18.9	18.4	2.71	0.50 hours

bridge are not completely the simple torsion or bending vibration. Sometimes, vibration shapes are overlaid results of two vibration shapes.

(2) In this paper, the experimental test was completed by the wireless sensor network technology. The tested time was too long, and parameters are too many, so that the collected data will be very huge, belonging to the category of big data. Then, experimental results and numerical simulation results are compared to perform the consistent changing trends. At some peaks, experimental values are slightly more than numerical simulation results. The reason is that boundary conditions of the numerical simulation are relatively ideal states and only consider effects of random traffic flow on the bridge, but they neglect practical wind excitation. In addition, material characteristics of numerical simulation can hardly be kept consistent with actual values. Wind speeds in experimental test are low, and excitation borne by the bridge is mainly generated from vehicles, so results between numerical simulation and experimental test do not have big errors. This result proves the reliability of the vehicle-bridge coupling model in the paper.

(3) The PSO-BP neural network model is used to predict vibration responses of the long-span bridge. Predicted values and real values of the neural network at each position point basically have the consistent changing trends, only some peak values are different, and the maximum error is less than 10%. Hence, it is feasible to predict vibration responses of the long-span bridge using the PSO-BP neural network model.

(4) In order to verify advantages of the prediction model, it is compared with the BP neural network model and GA-BP neural network model. The PSO-BP neural network model converges to the set critical error after it is iterated to the 226th generation, while the other two neural network models are not converged. The reason is that PSO can accelerate convergence of the neural network model. The training errors are 0.08 and 0.016, respectively, when the BP neural network reaches the maximum iteration 500, and GA-BP neural network reaches the 398th generation, but errors using the BP neural network are still more than the set critical error 0.016. In addition, the relative error of predicted values of PSO-BP neural network is only 2.71%, which is obviously less than the predicted results of other two neural network models. We can find that application of the PSO-BP neural network model proposed by the paper in predicting vibration responses is highly efficient and accurate.

Data Availability

The data used to support this study is currently under embargo while the research findings are commercialized. Requests for data, 6 months after publication of this article, will be considered by the corresponding author.

Conflicts of Interest

The authors declare that they have no conflicts of interest regarding this work.

Acknowledgments

This work is supported by the National Natural Science Foundation of China (51608137).

References

[1] J. Zhu, C. Chen, and Q. Han, "Vehicle-bridge coupling vibration analysis based fatigue reliability prediction of prestressed concrete highway bridges," *Structural Engineering and Mechanics*, vol. 49, no. 2, pp. 203–223, 2014.

[2] J. Kim and J. P. Lynch, "Experimental analysis of vehicle–bridge interaction using a wireless monitoring system and a two-stage system identification technique," *Mechanical Systems and Signal Processing*, vol. 28, pp. 3–19, 2012.

[3] J. Zhu and Q. Yi, "Bridge-vehicle coupled vibration response and static test data based damage identification of highway bridges," *Structural Engineering and Mechanics*, vol. 46, no. 1, pp. 75–90, 2013.

[4] X. Kong, D. J. Wu, C. S. Cai, and Y. Q. Liu, "New strategy of substructure method to model long-span hybrid cable-stayed bridges under vehicle-induced vibration," *Engineering Structures*, vol. 34, pp. 421–435, 2012.

[5] A. González, E. J. OBrien, and P. J. McGetrick, "Identification of damping in a bridge using a moving instrumented vehicle," *Journal of Sound and Vibration*, vol. 331, no. 18, pp. 4115–4131, 2012.

[6] S. Q. Wu and S. S. Law, "Vehicle axle load identification on bridge deck with irregular road surface profile," *Engineering Structures*, vol. 33, no. 2, pp. 591–601, 2011.

[7] J. Li and S. S. Law, "Damage identification of a target substructure with moving load excitation," *Mechanical Systems and Signal Processing*, vol. 30, pp. 78–90, 2012.

[8] M. Şimşek, "Non-linear vibration analysis of a functionally graded Timoshenko beam under action of a moving harmonic load," *Composite Structures*, vol. 92, no. 10, pp. 2532–2546, 2010.

[9] Y. Shi, Y. F. Song, H. Sun, and X. P. Zhou, "Dynamic analysis method of vehicle-bridge coupling for complicated bridges based on ANSYS," *Journal of Tianjin University*, vol. 43, no. 6, pp. 537–543, 2010.

[10] W. Ji, L. Deng, and W. He, "Vehicle-bridge coupled vibration analysis and calculation of dynamic impact factor for the PC box-girder bridge with corrugated steel webs," *Journal of Vibration Engineering*, vol. 29, no. 6, pp. 1041–1047, 2016.

[11] J. B. Zhang, J. B. Liao, G. W. Tang, and W. T. Xu, "Dynamic response of a bridge considering its surface random roughness," *Journal of Vibration and Shock*, vol. 35, no. 7, pp. 214–219, 2016.

[12] X. F. Yin and L. Deng, "Impact factor analysis of bridges under random traffic loads," *Journal of Hunan University (Natural Science)*, vol. 42, no. 9, pp. 68–75, 2015.

[13] X. F. Yin, J. M. Feng, Y. Liu, and C. S. Cai, "Vibrations of a long-span suspension bridge under stochastic traffic flows," *Journal of Hunan University (Natural Science)*, vol. 44, no. 1, pp. 47–53, 2017.

[14] S. R. Chen and J. Wu, "Modeling stochastic live load for long-span bridge based on microscopic traffic flow simulation," *Computers & Structures*, vol. 89, no. 9-10, pp. 813–824, 2011.

[15] B. Enright and E. J. O'Brien, "Monte Carlo simulation of extreme traffic loading on short and medium span bridges," *Structure and Infrastructure Engineering*, vol. 9, no. 12, pp. 1267–1282, 2013.

[16] K. Cui, W. Yang, and H. Gou, "Experimental research and finite element analysis on the dynamic characteristics of concrete steel bridges with multi-cracks," *Journal of Vibroengineering*, vol. 19, no. 6, pp. 4198–4209, 2017.

[17] P. Múčka, "Longitudinal road profile spectrum approximation by split straight lines," *Journal of Transportation Engineering*, vol. 138, no. 2, pp. 243–251, 2011.

[18] S. Ammanagi and C. S. Manohar, "Optimal cross-spectrum of road loads on vehicles: theory and experiments," *Journal of Vibration and Control*, vol. 22, no. 19, pp. 4012–4024, 2016.

[19] Y. Liu, G. Wang, Y. Yang, L. Jian, and S. Li, "Road surface equivalent reconstruction based on measured road spectrum," *Transactions of the Chinese Society of Agricultural Engineering*, vol. 28, no. 19, pp. 26–32, 2012.

[20] P. Múčka, "Current approaches to quantify the longitudinal road roughness," *International Journal of Pavement Engineering*, vol. 17, no. 8, pp. 659–679, 2016.

[21] C. S. Dharankar, M. K. Hada, and S. Chandel, "Numerical generation of road profile through spectral description for simulation of vehicle suspension," *Journal of the Brazilian Society of Mechanical Sciences and Engineering*, vol. 39, no. 6, pp. 1957–1967, 2017.

[22] J. Li, L. Huang, Y. Zhou, S. He, and Z. Ming, "Computation partitioning for mobile cloud computing in a big data environment," *IEEE Transactions on Industrial Informatics*, vol. 13, no. 4, pp. 2009–2018, 2017.

[23] J. S. Wu, S. Guo, J. Li, and D. Zeng, "Big data meet green challenges: big data toward green applications," *IEEE Systems Journal*, vol. 10, no. 3, pp. 888–900, 2016.

[24] K. Yang, N. Yang, C. W. Xing, J. Wu, and Z. Zhang, "Space-time network coding with transmit antenna selection and maximal-ratio combining," *IEEE Transactions on Wireless Communications*, vol. 14, no. 4, pp. 2106–2117, 2015.

[25] Q. J. Shi, J. S. Wu, Q. C. Chen, W. Xu, and Y. Wang, "Optimum linear block precoding for multi-point cooperative transmission with per-antenna power constraints," *IEEE Transactions on Wireless Communications*, vol. 11, no. 9, pp. 3158–3169, 2012.

[26] W. Wei, H. Song, W. Li, P. Shen, and A. Vasilakos, "Gradient-driven parking navigation using a continuous information potential field based on wireless sensor network," *Information Sciences*, vol. 408, pp. 100–114, 2017.

[27] J. Li, S. He, Z. Ming, and S. Cai, "An intelligent wireless sensor networks system with multiple servers communication," *International Journal of Distributed Sensor Networks*, vol. 11, no. 8, Article ID 960173, 2015.

[28] F. Yu and X. Xu, "A short-term load forecasting model of natural gas based on optimized genetic algorithm and improved BP neural network," *Applied Energy*, vol. 134, pp. 102–113, 2014.

[29] Y. G. Sun, H. Y. Qiang, X. Mei, and Y. Teng, "Modified repetitive learning control with unidirectional control input for uncertain nonlinear systems," *Neural Computing and Applications*, pp. 1–10, 2017.

[30] K. Cui and X. Qin, "Virtual reality research of the dynamic characteristics of soft soil under metro vibration loads based on BP neural networks," *Neural Computing and Applications*, vol. 29, no. 5, pp. 1233–1242, 2018.

[31] R. J. Kuo, M. C. Shieh, J. W. Zhang, and K. Y. Chen, "The application of an artificial immune system-based back-propagation neural network with feature selection to an RFID positioning system," *Robotics and Computer-Integrated Manufacturing*, vol. 29, no. 6, pp. 431–438, 2013.

[32] B. H. M. Sadeghi, "A BP-neural network predictor model for plastic injection molding process," *Journal of Materials Processing Technology*, vol. 103, no. 3, pp. 411–416, 2000.

[33] Z. Xiao, S. J. Ye, B. Zhong, and C. X. Sun, "BP neural network with rough set for short term load forecasting," *Expert Systems with Applications*, vol. 36, no. 1, pp. 273–279, 2009.

[34] S. Li, L. J. Liu, and Y. L. Xie, "Chaotic prediction for short-term traffic flow of optimized BP neural network based on genetic algorithm," *Control and Decision*, vol. 26, no. 10, pp. 1581–1585, 2011.

[35] J. B. Park, Y. W. Jeong, J. R. Shin, and K. Y. Lee, "An improved particle swarm optimization for nonconvex economic dispatch problems," *IEEE Transactions on Power Systems*, vol. 25, no. 1, pp. 156–166, 2010.

[36] G. M. Ding, Z. H. Tan, J. S. Wu, J. Zeng, and L. Zhang, "Indoor fingerprinting localization and tracking system using particle swarm optimization and Kalman filter," *IEICE Transactions on Communications*, vol. E98.B, no. 3, pp. 502–514, 2015.

[37] A. Nickabadi, M. M. Ebadzadeh, and R. Safabakhsh, "A novel particle swarm optimization algorithm with adaptive inertia weight," *Applied Soft Computing*, vol. 11, no. 4, pp. 3658–3670, 2011.

[38] V. Roberge, M. Tarbouchi, and G. Labonté, "Comparison of parallel genetic algorithm and particle swarm optimization for real-time UAV path planning," *IEEE Transactions on Industrial Informatics*, vol. 9, no. 1, pp. 132–141, 2013.